Electronic Supplementary Material (ESI) for ChemComm.

Supporting Information

Ultrasensitive Aptamer-based SERS Detection of Cancer Biomarker by Heterogeneous Core-Satellite Nanoassemblies

Materials.

Thiolated DNA aptamer was purchased from Shanghai Sangon Biological Engineering Technology & Services Co. Ltd. The aptamer was purified by high-performance liquid chromatography (HPLC) and suspended in deionized water from a Milli-Q device (18.2 MΩ, Millipore, Molsheim, France). Hydrogen tetrachloroaurate trihydrate ($HAuCl_4 \bullet 3H_2O$), sodium citrate, $AgNO_3$ were bought from Sigma-Aldrich and used as received. All glassware was soaked in aqua regia with 24 h for clearance, then rinsed at least three times with deionized water and dried in an oven.

Gold@silver core-shell nanoparticle synthesis

Using 17 nm Au NPs as seeds, Ag shell with 10 nm thick was deposited via the chemical reduction of Ag NO_3 with 700 μL of 0.1 M ascorbic acid. Au NPs with a uniform diameter of 17 nm were easily obtained, and larger NPs with perfect size and shape were difficult to obtain. The volume of ascorbic acid used was optimized according to the homogeneity of obtained core-shell nanoparticles, and more rod-shaped structures appeared when the amount of ascorbic acid was greater than 700 μL. Therefore, a total diameter of 37 nm Au@Ag NPs were selected as the SERS substrates,

DNA functionalized nanopartilcles

Aqueous dispersions (10 mL) of 10 nM NPs were stirred with excess BPS (40 mg/mL) at room temperature for 10 h. The dispersion was concentrated by centrifuging at 13,000 rpm for 10 min. The supernatants were removed and the resulting pellets were resuspended in 0.5×TBE buffer.

The modification of DNA onto the NPs performed in a 100 μL reaction system, and the buffer solution used was 0.01 M Tris-HCl containing 50 mM NaCl (pH 7.4). The core NP was adjusted to the concentration of 2 nM, and the DNA aptamer at a final concentration of 60 nM was then added. The 10 nm Au NPs at a concentration of 20 nM were reacted with 40 nM complementary DNA. After incubation for more than 8 h, the excess DNA in the two types of NPs was removed by centrifugation (two times) at 6500 rpm and 10000 rpm, respectively. The particles were resuspended in 0.01 M Tris-HCl and characterized by dynamic light scattering (DLS) to determine the change in NP size following modification with DNA. The hydrodynamic size of the DNA-modified NPs increased, which demonstrated

that DNA was successfully conjugated to the surface of the particles and could be used for the subsequent assembly of core-satellite nanostructures (Fig. S3).

Characterization

Transmission electron microscopy images were obtained using a transmission electron microscope (TEM, JEOL JEM-2100) operating at an acceleration voltage of 200 kV. 7 μL of the samples was dried in air dispersed onto a copper grid coated with the carbon film before the TEM characterization. The dynamic light scattering (DLS) data were measured using a Zetasizer Nano ZS system (Malvern) with 632.8 nm laser and a backscattering detector at 173°. All UV-Vis results were acquired on a UNICO 2100 PC UV-Vis spectrophotometer (200-800 nm) in a quartz cell and processed with the Origin Lab software. Raman scattering spectra were measured in liquid cell using a LabRam-HR800 Micro-Raman spectrometer with Lab-spec 5.0 software. The slit and pinhole were set at 100 and 400 mm, respectively, an air-cooled He-Ne laser for 532.8 nm excitation with a power of ~8 mW.

Computer Simulations of E-fields of core-satellite assemblies

Field enhancement properties of core-satellite assemblies were calculated by finite integration technique (FIT) method. An FIT package from CST STUDIO SUITE 2010 based on Maxwell's curl equations was used for the calculation in the vicinity of the plasmonic for media with electrical permittivity of ε=1. The core-satellite assemblies were modeled by 10 nm diameter Au NPs and 37 nm core-shell NPs separated by a gap of 8 nm. The electric fields were calculated for 632.8 nm excitation.

The calculation of limit of detection (LOD) for our assay:

The LOD was estimated without PSA giving SERS signal at least three times higher than background. The standard curve of PSA was plotted as

$$Y = A + B \times X \quad (1)$$

Where A and B are the variable obtained via least-square root linear regression for the signal-concentration curve for variable Y representing the SERS signal at PSA concentration of X (fM). In this study, A is 1012.3 and B is -826.3, respectively.

When

$$Y = Y_{blank} + 3SD \quad (2)$$

Where *SD* is the standard deviation and Y_{blank} is the SERS signal of blank sample (without PSA).

The LOD was calculated as

$$LOD = 10^{\frac{\left(Y_{blank} + 3SD\right) - A}{B}} \quad (3)$$

SD was calculated according to the well-known formula:

$$SD = \sqrt{\frac{1}{N-1} \times \sum_{i=1}^{N} (X_i - X_{average})^2} \quad (4)$$

where *N* is the total number of the PSA standard sample. X_i is the "i" sample of the series of measurements. $X_{average}$ is the average value of the SERS signals obtained for the specific series of identical samples repeated *N* times.

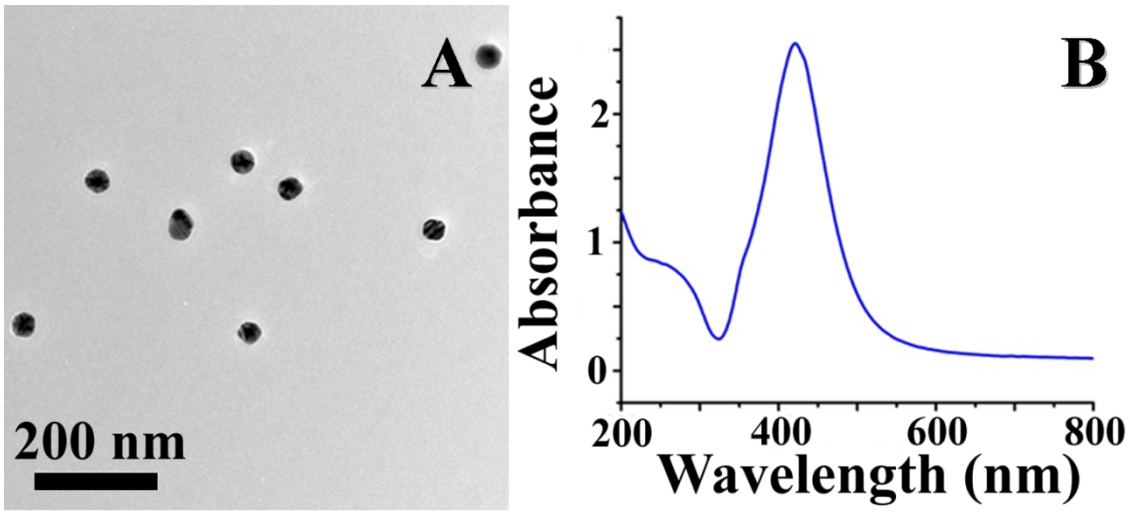

Fig. S1 Representative TEM image (A) and UV-Vis spectra (B) of 37 nm Au@Ag nanoparticles (NPs).

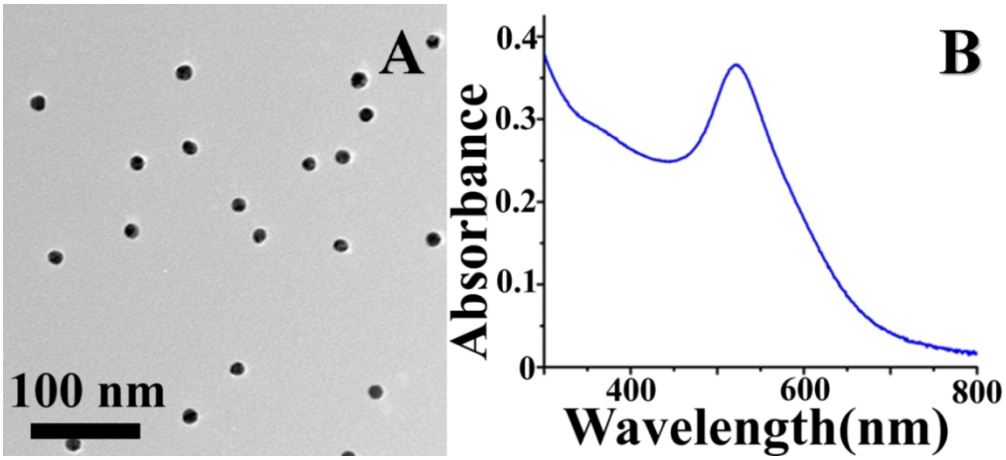

Fig. S2 Representative TEM image (A) and UV-Vis spectra (B) of 10 nm Au NPs.

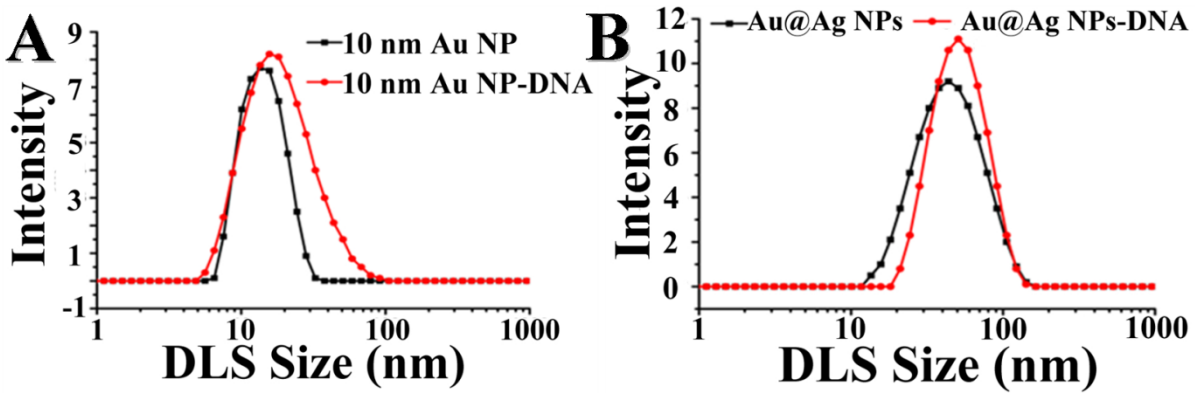

Fig. S3 DLS size change of 10 nm Au NPs and 17 nm Au@Ag NPs before and after DNA conjugation. (A) 10 nm Au NPs. (B) 37 nm Au@Ag NPs.

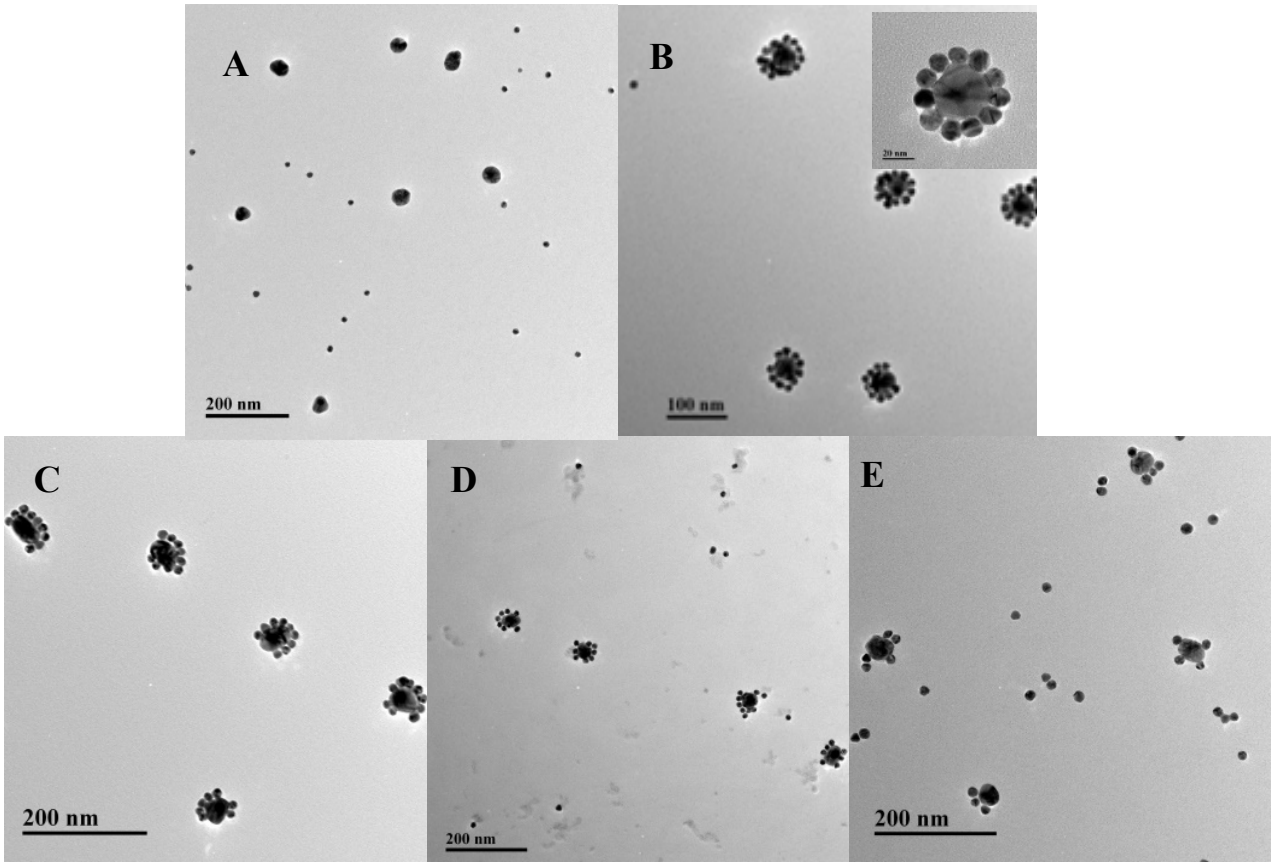

Fig. S4 Typical TEM images of core-satellite assemblies under different PSA concentrations and the mixture of individual NPs were included: (A) the mixture of Au@Ag NPs and Au NPs, (B) 0 fM, (C) 0.01 fM, (D) 0.5 fM, (E) 5 fM

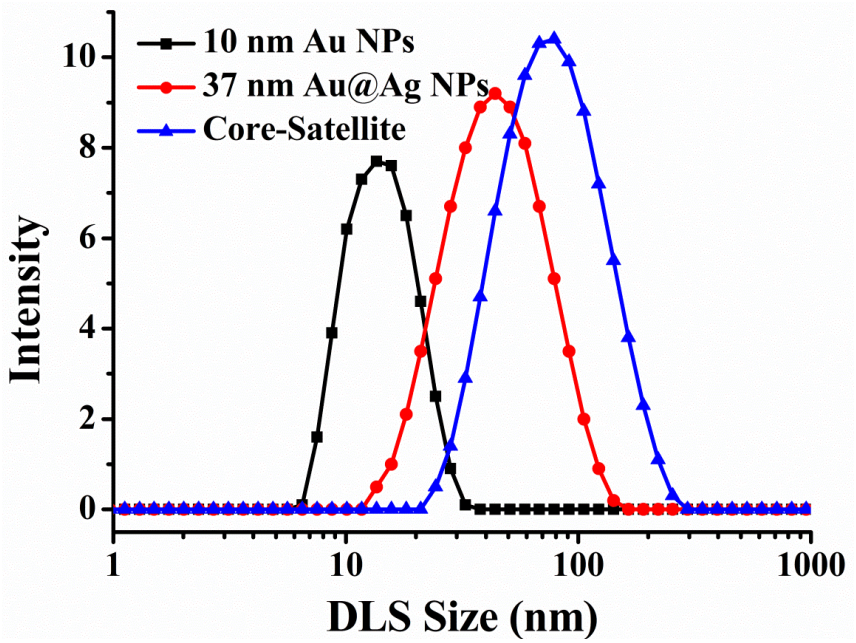

Fig. S5 DLS size change of core-satellite assemblies compared with individual NPs.

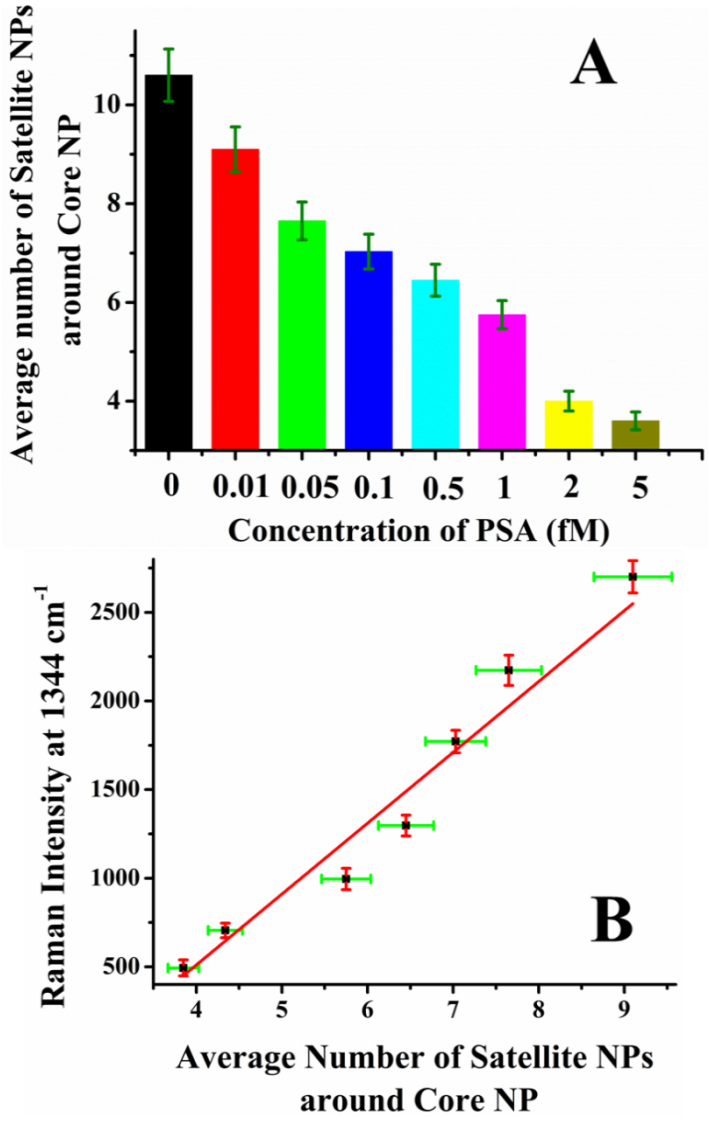

Fig. S6 (A) The average number of satellite NPs around core NP with different concentrations of PSA: 0, 0.01, 0.05, 0.1, 0.5, 1, 2 and 5 fM; (B) The correlation between Raman intensity at 1344 cm^{-1} and the average number of satellite NPs around core NP.

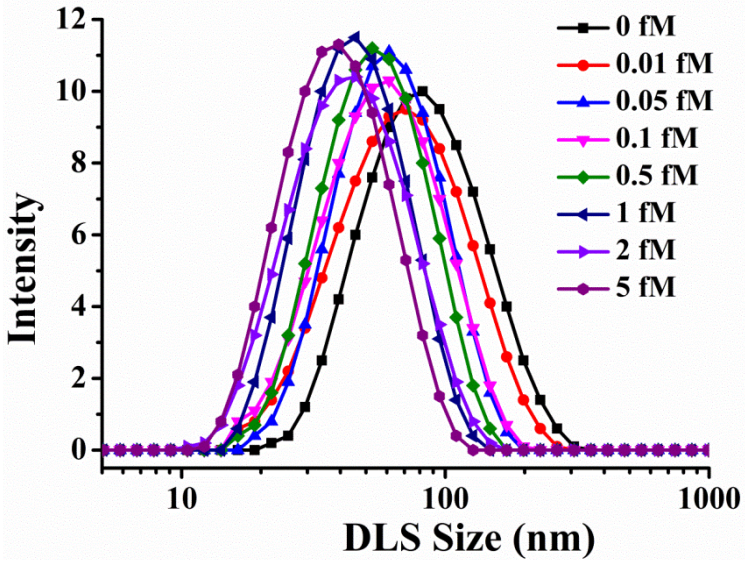

Fig. S7 DLS size distributions of assemblies under different concentrations of PSA in the range of 0 to 5 fM.

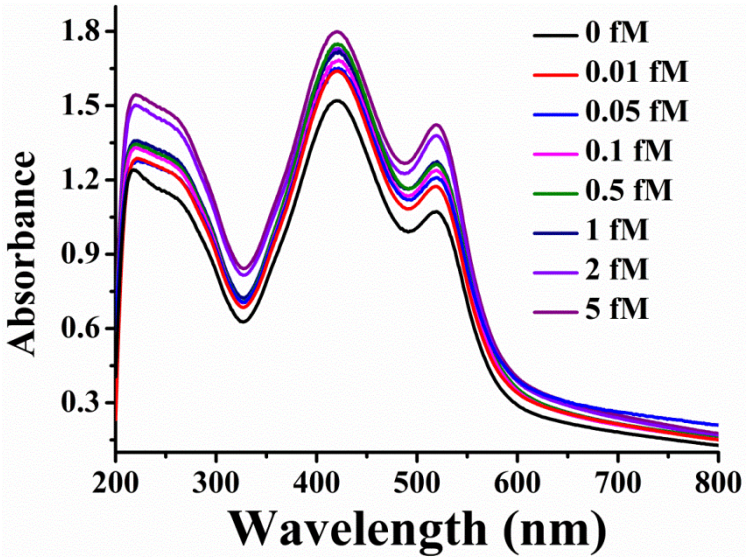

Fig. S8 UV-Vis spectra under different concentrations of PSA in the range of 0 to 5 fM.

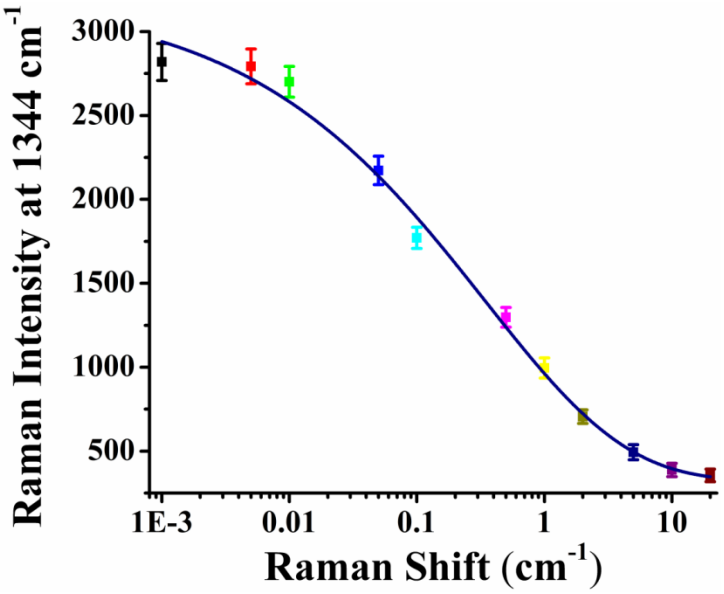

Fig. S9 Raman intensity at 1344 cm^{-1} in the range of 0.001 to 20 fM

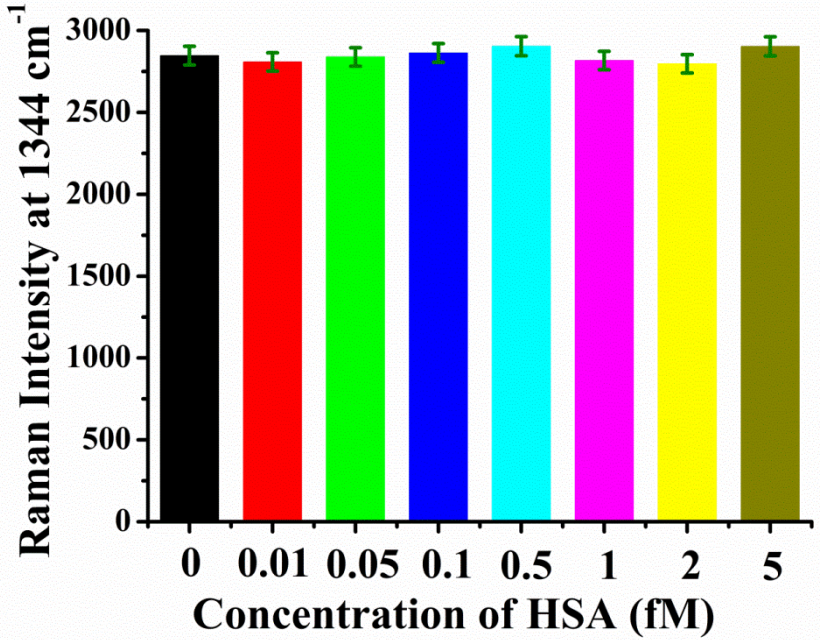

Fig. S10 The specificity of this method for the detection of HSA under the concentrations of 0, 0.01, 0.05, 0.1, 0.5, 1, 2 and 5 fM.

Tab. S1 Practical analysis of PSA in serum samples

Number of Sapmles[a]	Original Concentration (fM)[b]	Spiked Concentration (fM)	Detected Concentration Mean[c]±SD[d] (fM)	Recovery (%)
1	2.5	1.3	3.75±0.15	98.7
2	1.8	0.9	2.58±0.16	95.6
3	1.2	0.7	1.82±0.06	96.3
4	0.9	0.4	1.27±0.09	97.7
5	0.5	0.1	0.58±0.03	96.7
6	0.2	0.05	0.24±0.02	96.0

a. Serum sample NO.1to NO.6 are human sera, which are sampling from four healthy donors at the Second Hospital in Wuxi, China and then diluted to various concentrations including 2.5, 1.8, 1.2, 0.9, 0.5 and 0.2 fM.

b. Original concentrations of PSA in the sera were determined by the standard clinical diagnostic assay (ADVIA Centaur, Siemens).

c. The mean of three experiments;

d. SD=standard deviation